Modeling of Heat and Moisture Transfer in Porous Textile Medium Subject to External Wind: Improving Clothing Design

21

Nesreen Ghaddar and Kamel Ghali

Contents

Abstract

This chapter covers convective modeling approaches of heat and moisture transfer in textile materials coupled with human thermal response models. Fabrics are highly porous and relatively thin materials consisting mainly of solid fiber, adsorbed water vapor, and gaseous mixture of water vapor and air in the void space. Fabric ventilation is induced by external wind or body motion which causes the air to penetrate the fabric and transfer heat and water vapor away from the human skin to the environment.

N. Ghaddar (✉) · K. Ghali
Department of Mechanical Engineering, Faculty of Engineering and Architecture, American University of Beirut, Beirut, Lebanon
e-mail: farah@aub.edu.lb; ka04@aub.edu.lb

F. A. Kulacki (ed.), *Handbook of Thermal Science and Engineering*,
https://doi.org/10.1007/978-3-319-26695-4_40

Convective fabric models are developed to predict local and overall clothing ensemble ventilation rates. This modeling approach is combined with segmental bio-heat model to predict human local and overall comfort in hot humid environment. The integration of clothing ventilation models with “cylindrical” segments of the clothed human body is presented showing examples of how segmental and inter-segmental ventilation, sensible heat loss, and moisture transport through clothing are used to assess the whole body comfort.

Nomenclature

A_f	Area of the fabric (m^2)
A_i	Inner node area in contact with the outer node (m^2)
A_o	Outer-node exposed surface area to air flow (m^2)
C_a	Gas concentration in the micro-climate measurement location (m^3 Ar /m^3 air)
C_f	Fiber specific heat (J/kg K)
C_{in}	Gas concentration in the distribution system (m^3 Ar /m^3 air)
C_p	Specific heat of air at constant pressure (J/kg ·K)
C_v	Specific heat of air at constant volume (J/kg ·K)
D	Water vapor diffusion coefficient in air (m^2/s)
e_f	Fabric thickness (m)
g	Gravitational acceleration (m/s^2)
h_{ad}	Heat of adsorption (J/kg)
H'_{ci}	Normalized conduction heat transfer coefficient between inner node and outer node (W/m^2·K)
H'_{co}	Normalized convection heat transfer coefficient between outer node and air flowing through fabric (W/m^2·K)
$h_{c(f\text{-}\infty)}$	Heat transport coefficient from the fabric to the environment (W/m^2·K)
$h_{c(o\text{-air})}$	Heat transport coefficient from the fabric to the trapped air layer (W/m^2·K)
$h_{c(\text{skin-air})}$	Heat transport coefficient from the skin to the trapped air layer (W/m^2·K)
h_{fg}	Heat of vaporization of water (J/kg)
H'_{mi}	Normalized diffusion mass transfer coefficient between inner node and outer node (kg/m^2·kPa·s)
H'_{mo}	Normalized mass transport coefficient between outer node and air void in the fabric (kg/m^2·kPa·s)
$h_{m(f\text{-}\infty)}$	Mass transfer coefficient between the fabric and the environment (kg/m^2·kPa·s)
$h_{m(o\text{-air})}$	Mass transfer coefficient between the fabric and the air (kg/m^2·kPa·s)
$h_{m(\text{skin-air})}$	Mass transfer coefficient between the skin and the air layer (kg/m^2·kPa·s)
i_m	Permeability index
k_a	Thermal conductivity of air (W/m·K)

h_r	Linearized radiative heat transfer ($W/m^2{\cdot}K$)
L	Fabric length in z direction (m)
$\dot{m}_{aY}$	Mass flow rate of air in radial direction ($kg/m^2{\cdot}s$)
$\dot{m}_{a\theta}$	Mass flow rate of air in angular direction($kg/m^2{\cdot}s$)
$\dot{m}_{aZ}$	Mass flow rate of air in axial direction ($kg/m^2{\cdot}s$)
$\dot{m}_a$	Total ventilation rate ($kg/m^2{\cdot}s$)
P_a	Pressure of the microclimate air (kPa)
P_s	Pressure at the external surface of the fabric (kPa)
T_a	Temperature of the microclimate air (°C)
T_{amb}	Ambient temperature (°C)
T_{skin}	Skin temperature (°C)
T_o	Temperature of the fabric outer layer (°C)
T_v	Temperature of the fabric void layer (°C)
Q	Heat loss (W/m^2)
R	Total regain in fabric (kg of adsorbed H_2O/kg fiber)
R_D	Fabric dry resistance ($m^2{\cdot}K/W$ unless specified in the equation per mm of thickness)
R_E	Fabric evaporative resistance ($m^2{\cdot}kPa/W$)
$R_{dynamic}$	The dynamic resistance for ventilation through the fabric ($m^2{\cdot}K/W$)
R_f	Fabric cylinder radius (m)
R_s	Segment cylinder radius (m)
V	Liquid movement velocity (m/s)
V_∞	Velocities of the environment cross wind (m/s)
w	Humidity ratio (kg of water/kg of air)
Y	Air layer thickness (m)
z	Coordinate in vertical direction (m)

Greek Symbols

α	Fabric air permeability ($m^3/m^2{\cdot}s$)
β	The volumetric thermal expansion ($°C^{-1}$)
μ	Viscosity of air ($N{\cdot}s/m^2$)
θ	Angular coordinate
ε	Porosity of fabric
ρ_a	Density of air (kg/m^3)

Subscripts

a	Conditions of air in the annulus
fabric	Fabric
o	Fabric outer node
void	Fabric void node
skin	Conditions at the skin surface
∞	Environment condition

1 Introduction

Modeling transient mechanisms of coupled heat and moisture transfer into textile materials has been a topic of interest for many decades since clothing is a crucial parameter in determining human thermal comfort. In fact, the thermal comfort status of people is largely affected by the way the clothing mediates the flow of heat and moisture from the human skin to the environment through the mediating microclimate air layer between trapped between skin and fabric. Fabrics are highly porous and relatively thin materials consisting mainly of solid fiber, adsorbed water vapor, and gaseous mixture of water vapor and air in the void space. The porosity of most fabrics ranges from 50% to 95% depending on the fiber fineness, the tightness of the twist in the yarns, and the yarn count. Water vapor transport may take place by molecular diffusion due to gradients in the partial vapor pressure and by bulk transport due to convective air flow.

Models of clothing varied in complexity depending on fabric hygroscopic properties and applicability of the assumption of thermal and vapor concentration equilibrium between the solid fiber and its entrapped air voids. This chapter will review modeling approaches of clothing material and associated microclimate, focusing on convective heat and moisture transfer due to material ventilation induced by relative wind penetrating the fibrous medium. Convective fabric and clothed cylinder models have been used to predict local and overall clothing ensemble ventilation rates. This latter modeling approach has a wider applicability since it can be combined with segmental bio-heat models to predict human local and overall comfort in hot humid environment. The integration of clothing ventilation model with "cylindrical" segments of the clothed human body is presented showing examples of how segmental and inter-segmental ventilation, sensible heat loss, and moisture transport through clothing are used to assess the whole body comfort and hence improve clothing design. The chapter will end with a recommendations' section of best interventions for improving clothing performance in hot humid climate.

2 Review of Fabric Heat, Air, and Water Vapor Transport Models

Mathematical modeling of heat and mass transfer in porous media has been widely studied in the literature. Fabrics used in clothing systems, in particular, are highly porous thin material that allowed simplified modeling of heat and mass transfer by diffusion and convection. Thermal modeling of fabrics is important in evaluating clothed human thermal response and hence human thermal comfort. The heat exchange between human body and the environment is significantly affected by the way the clothing layers mediates the flow of heat and moisture from the human skin to the environment by diffusion in fabric and air layers and by ventilation induced by relative wind resulting in air penetration through the fabric to microclimate air trapped between skin and fabric. Models that consider heat and vapor transport through the clothing system when exposed to different environmental conditions and external wind will be considered in this section after discussing the most important fabric physical parameters that are used in these models.

2.1 Fabric Physical Parameters

Fabrics are highly porous and relatively thin materials made from fibers that have been spun into yarns that are used in weaving the fabric structure. The fabric system consists of the solid fiber matrix and void space. Water vapor can exist in both the adsorbed state in the solid fiber and in void air between the solid fibers, and liquid water can be present in the interstices of the fabric when subjected to wet conditions. Water vapor transport may take place by molecular diffusion due to gradients in vapor pressure and by bulk transport due to convective air flow. Liquid transport may occur by molecular diffusion caused by concentration gradients and by capillary forces as well as gravity. Energy transport occurs by conduction and by convective flows of all phases that are able to move.

Predicting the heat and mass transfer in fabric system is a complex task and cannot be accomplished without the input information of the transfer properties. The following physical properties are important when considering modeling of heat and moisture transfer in fabrics:

2.1.1 Air Permeability (α)

It can also be used to provide an indication of the breathability of fabrics. It is highly correlated to the yarn weave structure and the size of Micro pores inside the yarn and macropores between the yarns. It is usually determined by subjecting the fabric to a prescribed pressure difference and measuring the air flow rate passing perpendicularly to a fabric of a known cross-sectional area, ASTM D737-96 (2012). It is generally expressed in SI units as $cm^3/s/cm^2$.

2.1.2 Porosity

The fabric porosity "ε_f" is generally defined as the air ratio of the air volume in the fabric to the total volume of the fabric structure. It is expressed with Eq. 1 in terms of the corresponding densities:

$$\varepsilon_f = \left(1 - \frac{\rho_{\text{fabric}}}{\rho_{\text{fiber}}}\right) \tag{1}$$

where ρ_{fabric} and ρ_{fiber} are the densities of the fabrics (g/cm^3) and of the fiber (g/cm^3), respectively.

Fabric thickness: Fabric thickness is highly dependent on yarn diameter and the fabric weave and usually expressed in mm. Determination of thickness of fabric samples is usually determined using a precision thickness gauge. The fabric sample is placed horizontally on a circular anvil without any tension and a standard load of 3.4 lbs./sq. in is pressed on the fabric specimen, ASTM D-39-49 (1965).

2.1.3 Wetting and Wickability of Fabrics

Textile researchers distinguish between two phenomena related to liquid transport in fabrics, the wettability and the wickability. Each term addresses a different application of a fabric that is brought in contact with liquid. Harnett and Mehta (1984) gives the following definitions "*Wickability is the ability to sustain capillary flow*" whereas wettability "describes the initial behavior of a fabric, yarn, or fiber when brought into contact with water." While wetting and wicking refer to what appear to be separate phenomena, they can be described by a single process. In wetting, the fabric is initially dry but the liquid must still move through the fabric in order to spread and be soaked up by the fabric. In wicking, a continuous liquid phase is present. There is no sharp distinction between wetting and wicking. At some point during wetting, the fabric becomes sufficiently saturated that the process becomes wicking. Fabrics are normally weaved as a homogenous medium in their structure (porosity, permeability) and thin in their thickness. Moisture movement in fabrics is generally slow and if the flow does not affect the pore fabric size, then the moisture transport can be described by Darcy law and liquid velocity V is then given by

$$V = \frac{\alpha}{\mu}\frac{dP_c}{dx} \tag{2}$$

Where α is the permeability which describes the ease with which water liquid flows through the porous media, μ is the viscosity of the advancing liquid, and P_c is capillary pressure which is the driving force for the liquid movement.

Ghali et al. (1994) used a variation of the "long column" to measure the capillary pressure of long strips of fabrics suspended vertically above a container of water with the bottom end immersed. Ghali et al. (1995) expressed the capillary pressure function of the fabric degree of saturation. As for the permeability, they used the siphon to measure the permeability function of saturation, and they proposed a new transient measuring technique for determining permeability.

2.1.4 Dry and Evaporative Resistance of Fabrics

Steady heat and mass transport from clothing systems were based on dry and evaporative resistances of the fabric. The basic energy balance for dry heat flow is given by

$$Q_D = A\frac{T_{\text{skin}} - T_{\text{env}}}{R_D} \tag{3}$$

where Q_D (W/m^2) is the dry heat transfer and takes place across the clothing layer between the skin and the environment, A (m^2) is the clothing surface area, T_{skin} is the skin temperature, T_{env} is the environment temperature, and R_D is the total resistance of the fabric layer. The dry resistance of the fabric is dependent upon the amount of still air entrapped in the interstices between the fibers and yarns since the conductivity of air is much lower than that of fiber materials (Fourt and Hollies 1970). The solid fibers arrangement and their volume in the fabric influence the fabric insulation more than the fiber itself (Rees 1941). Any fabric characteristics that would increase the amount of still air in the fabric would also increase its dry resistance. Thermal resistance of the fabric is usually negatively correlated with fabric density. The dry heat resistance for indoor worn fabrics is reported by McCullough et al. (1985, 1989) as follows:

$$R_D = 0.015 \times e_f \tag{4}$$

where R_D is the dry resistance of the fabric in $m^2 \cdot K/mm \cdot W$ and e_f is the fabric thickness in mm.

Similarly the evaporative heat flow Q_E is given by

$$Q_E = A \frac{P_{\text{skin}} - P_{\text{env}}}{R_E} \tag{5}$$

where R_E is the total evaporative resistance of the clothing layer, P_{skin} is the water vapor pressure at the skin, and P_{env} is the water vapor pressure in the environment. Similar to dry heat transfer, vapor transfer in fabrics depends on the physical properties of the entrapped air medium and on the arrangement of the solid fibers. The solid fibers not only absorb/desorb moisture but they also represent an obstacle for the vapor molecules on their way through the fabric (Chatterjee 1985). Therefore, the vapor resistance of fabrics is expected to be larger than that of equally thick air layer and is expressed as an equivalent thickness of still air that would give the same resistance to vapor transfer as that of the actual fabric. This equivalent air thickness was found by McCullough et al. (1989) to increase linearly with the fabric thickness for low-density fabrics and to some extent for dense fabric materials.

The dry and evaporative resistances are also related through the permeability index, i_m, which was first proposed by Woodcock (1962). The relationship is expressed by

$$i_m = (R_D/R_E)LR \tag{6}$$

where R_E is the evaporative resistance of the fabric in $m^2 \cdot kPa/W$ and LR is the Lewis ratio equals approximately 16.65 K/kPa at typical indoor conditions.

The heat transfer through a textile layer is a complex combination of conduction, radiation, and convection. However, it is rather common to use the total thermal resistance of textile medium instead of evaluating thermal processes. The thermal resistance for the clothing system is obtained by summation of each individual fabric and air layer of the clothing system. Thermal and evaporative resistances for each individual fabric sample can be measured using dry and sweating hot plate in accordance to ASTM D 1518 (1985) and ISO 11092 (1993), respectively.

2.1.5 Dynamic Dry and Evaporative Resistances of Fabric Subject to Normal Flow

Ventilation causes a dynamic change of clothing insulation due to wind penetration through fabric or ensemble openings, wearer displacement due to motion causing a wind effect, and relative motion of clothed body parts (limbs) with respect to their clothing cover. The fabric static dry and evaporative resistances are corrected for normal flow rate through the fabric denoted as $\dot{m}_{aY}$. The normal airflow passing through thin fabric at constant fabric permeability is given by (Lotens 1993):

$$\dot{m}_{aY} = \frac{\alpha \rho_a}{\Delta P_m}(P_a - P_\infty) \tag{7}$$

where $\dot{m}_{aY}$ is the flow rate through fabric normal to the fabric surface, α is the fabric air permeability in m^3/m^2·s, $\Delta P_m = 0.1245$ kPa from standard tests on fabrics' air permeability (ASTM D737-75 1983), P_a is the air pressure in the microclimate trapped air layer between the human skin and the fabric (kPa), and P_∞ is the outside environment air pressure (kPa).

The dynamic dry resistance of the clothing is given by (Havenith et al. 1990, 2000; Ghali et al. 2009):

$$R_{D,\text{dynamic}} = \frac{1}{\left(\frac{1}{R_D} + \dot{m}_{aY} Cp_a\right)} \tag{8}$$

where $R_{D,\text{dynamic}}$ is the dynamic dry resistance for ventilation through the fabric and Cp_a is the penetrating air specific heat. The dynamic resistance is a parameter to correct for ventilation effect on clothing static resistance at no wind. Similarly, the dynamic evaporative fabric resistance is given by

$$R_{E,dynamic} = \frac{1}{\left(\frac{1}{R_E} + \frac{1}{\left(\frac{\rho_a R_{H_2O} T_\infty}{\dot{m}_{aY} h_{ad}}\right)}\right)} \tag{9}$$

where R_{H_2O} is the water vapor gas constant, ρ_a is the air density, T_∞ is the penetrating air temperature, and h_{ad} is the fabric water-vapor heat of adsorption.

2.2 Diffusive and Convective Fabric Models

The first clothing model that describes the mechanism of transient diffusion of heat and moisture transfer into an assembly of hygroscopic textile materials was introduced and analysed by Henry (1939). He developed a set of two differential coupled governing equations for the mass and heat transfer in a small flat piece of clothing material. Henry's analysis was based on a simplified analytical solution. In order to describe the complicated process of adsorption behavior in textile materials, Nordon and David (1967) presented a model in terms of experimentally adjustable parameters appropriate for a first stage of rapid moisture sorption followed by a second stage of slow moisture sorption. However, their model did not take into account the physical mechanisms of the sorption process. For this reason, Li and Holcombe (1992) introduced a new two-stage adsorption model to better describe the coupled heat and moisture transport in fabrics. Moreover, Farnworth (1986) developed a numerical model that took into account the condensation and adsorption in a multilayered clothing system. Jones and Ogawa (1993) developed another new unsteady-state thermal model for the whole clothing system. The whole clothing system model was based on simplified expressions of Henry's model. Li and Holcombe (1992) presented a transient mathematical clothing model that describes the dynamic heat and moisture transport behavior of clothing and human body.

The abovementioned models assumed instantaneous equilibrium between the local relative humidity of the penetrating air and the moisture content of the fiber. However, the hypothesis of local equilibrium was shown to be invalid during periods of rapid transient heating or cooling in porous media as reported by Minkowycz et al. (1999). In the absence of local thermal equilibrium, the solid and fluid should be treated as two different constituents. Under vigorous clothed human movement of a relatively thin porous textile material or with clothing exposure to external wind, the air will pass quickly between the fibers, invalidating the local thermal equilibrium assumption. The ventilation rate was affected mainly by the walking velocity as described by Lotens (1993) who derived empirically the steady clothing ventilation rate as function of the air permeability of the fabric and the effective wind velocity. Ghali et al. (2002a) developed a two-node fabric absorption model using empirically predicted transfer coefficients of a cotton fibrous medium to account for the state of nonthermal equilibrium between solid fiber and air passing through the fabric void space. They extended their model of the fiber to include modeling of the microclimate air in the voids of the fabric and predict the change of air temperature across the fiber (Ghali et al. 2002b, c). They also considered the periodic movement of clothed limbs on renewal of trapped air between clothing and skin by flowing through the fabric void space and clothing apertures. The advantage of the non-equilibrium thin fabric models is that they can be combined with ventilation models estimating the renewal rate of the microclimate air in the gap between skin and clothing. This facilitates the integration with human thermal bio-heat models.

In the next sections, the thin fabric model is derived and it is then combined with the microclimate air clothed cylinder ventilation model for effective use in many applications related to human thermal comfort. The combined model is integrated with bio-heat models to predict clothed human thermal response and associated comfort as a function of clothing, activity level, and environmental parameters.

3 Mathematical Formulation of Thin Fabric Model for Clothing Ventilation Applications

The fabric model presented here is based on Ghali et al. (2002b) while using a lumped layer of two fabric nodes and an air void node to represent the fibrous medium. The model is simple and is applicable to highly permeable thin fabrics. Lumped parameters have commonly been used in models of thin permeable fabrics (Farnworth 1986; Jones and Ogawa 1993).

The three-node model lumps the fabric into an outer node, inner node, and an air void node. The fabric outer node represents the exposed surface of the yarns, which is in direct contact with the penetrating air in the void space (air void node) between the yarns. The fabric inner node represents the inner portion of the "solid" yarn, which is surrounded by the fabric outer node. The outer node exchanges heat and moisture transfer with the flowing air in the air void node and with the inner node, while the inner node exchanges heat and moisture by diffusion only with the outer node. The air flowing through the fabric void spaces does not spend sufficient time to be in thermal equilibrium with the fabric inner and outer nodes. The moisture uptake in the fabric occurs first by the convection effect from the air in the void node to the yarn surface (outer node), followed by sorption/diffusion to the yarn interior (inner node). The fabric model is best represented by a flow of air around cylinders in cross flow, where the air voids are connected between the cylinders (yarns) as shown in Fig. 1. The fabric is represented by a large number of these three-node modules in cross flow depending on the fabric effective porosity. The fabric area is $L \times W$ and the fabric thickness is e_f. The airflow is assumed normal to the fabric plane. In the derivation of the water vapor mass balances in the outer node, inner node, and the air void node, the water vapor is assumed very dilute compared to the air and the bulk velocity of the mixture is very

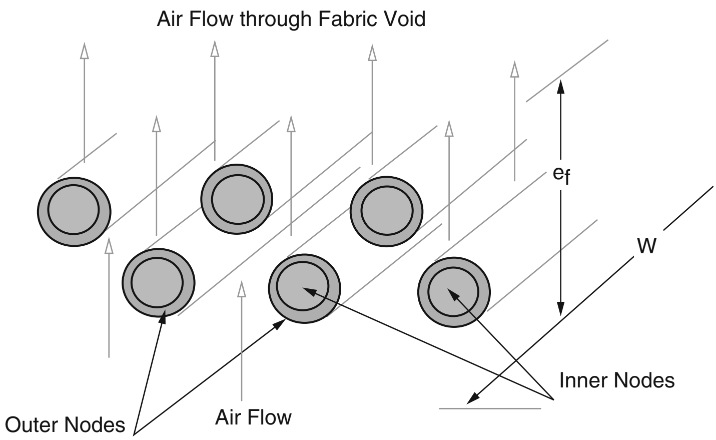

Fig. 1 Schematic of lumped fabric three-node model

close to the velocity of the air. The second main assumption is that the volume changes of fibers due to sorption process are small enough to be neglected.

Effective heat and mass transfer coefficients, reported by Ghali et al. (2002a, b), H_{co} and H_{mo} for the outer node of the fabric, and the heat and mass diffusion coefficients H_{ci} and H_{mi} for the inner nodes of the fabric, were used in the model in normalized form as follows:

$$H'_{mo} = H_{mo}\frac{A_o}{A_f}, \quad H'_{co} = H_{co}\frac{A_o}{A_f}, \quad H'_{mi} = H_{mi}\frac{A_i}{A_f}, \quad H'_{ci} = H_{ci}\frac{A_i}{A_f} \tag{10}$$

where A_f is the overall fabric surface area, A_o is the outer-node exposed surface area to air flow and A_i is the inner node area in contact with the outer node. The values of these normalized convection coefficients for cotton fabric are given by (Ghaddar et al. 2005)

$$H'_{Co} = 495.72\dot{m}_{aY} - 1.85693 \qquad \mathrm{W/m^2 \cdot K}, \quad \dot{m}_{aY} > 0.00777\mathrm{kg/m^2 \cdot s} \tag{11a}$$

$$H'_{Co} = 2.0 \qquad \mathrm{W/m^2 \cdot K}, \quad \dot{m}_{aY} \leq 0.00777\mathrm{kg/m^2 \cdot s} \tag{11b}$$

$$H'_{mo} = 3.408 \times 10^{-3}\, \dot{m}_Y - 1.2766 \times 10^{-5}\ \mathrm{kg/m^2 \cdot kPa \cdot s}, \ \dot{m}_{aY} > 0.00777\ \mathrm{kg/m^2 \cdot s} \tag{11c}$$

$$H'_{mo} = 1.3714 \times 10^{-5} \qquad \mathrm{kg/m^2 \cdot kPa \cdot s}, \ \dot{m}_{aY} \leq 0.00777\mathrm{kg/m^2 \cdot s} \tag{11d}$$

where the normal air flow rate is as defined in Eq. 7 as a function of the fabric air permeability. The inner node transport coefficients to be used in the fabric model are as reported by Ghali et al. (2002a) at $H'_{ci} = 1.574$ W/m^2·K, and $H'_{mi} = 7.58 \times 10^{-6}$ kg/m^2·kPa·s.

The time-dependent mass and energy balances are for the outer and inner nodes of the fabric yarn and of the air void node in terms of the heat and mass transport coefficients between the penetrating air and the outer node and between inner and outer node. In the derivation of the water vapor mass balances in the fabric and void space nodes, the water vapor is assumed dilute compared to the air and the bulk velocity of the mixture is very close to the velocity of the air. This assumption simplifies the mass balances by ignoring the effect of counter transfer of the air and assuming constant total pressure of the system. According to ASHRAE Handbook of Fundamentals (2005), no appreciable error is introduced when diffusion of a dilute gas through an air layer is done. The derivation included a term to correct for bulk motion of the fluid and its value is typically between 1.00 and 1.05 for conditions of the ventilating air. The water vapor mass balance in the air void node is given in Eqs. 12a and b when air flow enters the fabric void from the environment space to the microclimate layer ($P_a < P_\infty$) and when air flow enters the fabric void space from the microclimate layer to the environment ($P_a > P_\infty$), respectively, as

$$\frac{\partial}{\partial t}\left(\rho_a e_f w_{\text{void}} \varepsilon_f\right) = -\dot{m}_{ay}\left[w_p - w_{\text{void}}\right] + H'_{mo}[P_o - P_a] + D\frac{\rho_a(w_a - w_{\text{void}})}{e_f/2} + D\frac{\rho_a(w_\infty - w_{\text{void}})}{e_f/2} \tag{12a}$$

where

$$w_p = \begin{cases} w_\infty & P_a < P_\infty \\ w_a & P_a \geq P_\infty \end{cases} \tag{12b}$$

where ε_f is the fiber porosity. The last two terms in equations are the mass diffusion terms within the fabric in angular and axial directions. The outer fiber node and the inner fiber node mass balances are expressed in terms of the fabric regain in Eqs. 13a and b, respectively

$$\frac{dR_o}{dt} = \frac{1}{\rho\gamma e_f}\left[H'_{mo}(P_{\text{void}} - P_o) + H'_{mi}(P_i - P_o)\right] \tag{13a}$$

$$\frac{dR_i}{dt} = \frac{H'_{mi}}{\rho(1-\gamma)t_f}[P_o - P_i] \tag{13b}$$

where R_o is the regain of the outer node (the mass of moisture adsorbed by fiber outer node divided by dry mass of the fiber outer node), R_i is the regain of the inner node, and H'_{mo} and H'_{mi} are the mass transfer coefficients between the outer node and the penetrating air and the outer node and the inner node, respectively. The parameter γ is the fraction of mass that is in the outer node and it depends on the fabric type and the fabric porosity. The total fabric regain R (kg of adsorbed H_2O/kg dry fiber) is given by

$$R = \gamma R_o + (1-\gamma)R_i \tag{14}$$

According to the model of Ghali et al. (2002a), the value of γ is equal to 0.6. The energy balance for the air vapor mixture in the air void node is given by

$$\varepsilon_f\frac{\partial}{\partial t}\left[\rho_a e_f\left(C_v T_{void} + h_{fg} w_{void}\right)\right] = -\dot{m}_{ay}[H_e] + \dot{m}_{ay}\left[C_p T_{\text{void}} + w_{void} h_{fg}\right] + H'_{co}[T_o - T_{void}] + k_a\frac{T_a - T_{void}}{e_f/2} + k_a\frac{T_\infty - T_{void}}{e_f/2} + Dh_{fg}\frac{\rho_a(w_a - w_{void})}{e_f/2} + Dh_{fg}\frac{\rho_a(w_\infty - w_{void})}{e_f/2} \tag{15a}$$

where H_e is given by

$$H_e = \begin{cases} C_p T_\infty + w_\infty h_{fg} & \text{for} \quad P_a < P_\infty \\ C_p T_a + w_a h_{fg} & \text{for} \quad P_a \geq P_\infty \end{cases} \tag{15b}$$

The heat transfer coefficient between the outer node and the penetrating air in the voids is H'_{co} and k_a is the thermal conductivity of air. The last four terms of the energy balance are heat diffusion term in axial and angular directions. These terms are negligible when only normal flow through the fabric is present.

The energy balance on the outer nodes gives

$$\rho_f(1-\gamma)\left[C_f\frac{dT_o}{dt}-h_{ad}\frac{dR_o}{dt}\right]=\frac{H'_{co}}{e_f}[T_{\text{void}}-T_o]-\frac{H'_{ci}}{e_f}[T_o-T_i]+\frac{h_r}{2e_f}(T_{\text{skin}}-T_o)+\frac{h_r}{2e_f}(T_\infty-T_o) \quad (16)$$

where H'_{ci} is the heat diffusion coefficient between the outer node and the inner node, h_r is the linearized radiative heat exchange coefficient, and h_{ad} is the enthalpy of the water adsorption state. The density of the adsorbed phase of water is similar to that of liquid water. The high density results in the enthalpy and internal energy of the adsorbed phases being very nearly the same. Therefore, the internal energy, u_{ad}, can be replaced with the enthalpy of the adsorbed water. Data on h_{ad}, as a function of relative humidity, is obtained from the work of Morton and Hearle (1975).

The energy balance on the inner node gives

$$\rho_f\gamma\left[C_f\frac{dT_i}{dt}-h_{ad}\frac{dR_i}{dt}\right]=\frac{H'_{ci}}{e_f}[T_o-T_i] \quad (17)$$

The above-coupled differential Eqs. 12a, b, 13a, b, 14, 15a, b, 16 and 17 describe the time-dependent convective mass and heat transfer from the skin-adjacent air layer through the fabric induced by the sinusoidal motion of the fabric. To solve the equations for the fabric transient thermal response, the fabric void microscopic transport coefficients, namely, H'_{mo}, H'_{co}, and the inner node diffusion coefficients H'_{mi} and H'_{ci}, and the internal convection coefficients from the skin to the air layer $h_{m(\text{skin-}a)}$ and $h_{(\text{skin-}a)}$ must be known.

4 Integration of Thin Fabric Model with Segmental Clothed Human Thermal Model

One of the important applications of the thin fabric model is clothing ventilation for prediction of clothed human heat loss when subject to external wind or relative wind due to walking. Predicting segmental clothing ventilation is important for improving garment design by modifying design parameters to enhance or decrease local ventilation rate depending on the type of clothing including protective clothing. This is why researchers have been interested in developing mathematical models from the first principles to predict local clothing ventilation.

Modeling approach has mainly been based on representing the human body as a number of independent cylindrical segments covered with garment material in cross air flow (Ismail et al. 2014; Othmani et al. 2008).

The clothed human body can be constructed a number of connected or disconnected clothed cylinders. These segments or cylinders are typically the clothed two arms, the clothed two legs, and the clothed trunk as shown in Fig. 2. Each segment consists of two concentric vertical cylinders for standing or walking person. The outer cylinder representing the fabric covers the inner heated cylinder representing the human skin (Ghaddar et al. 2010). The human skin temperature can be obtained from integration with a bio-heat model that simulates the human thermal response based on physiology and heat and mass transfer mechanisms that take place at the skin and through respiration (Ghaddar et al. 2008; Ismail et al. 2014). Mathematical modeling of clothed limbs and trunk would also require consideration of the air annulus between the human skin and the clothing. Clothing apertures are most likely to be at the top for the trunk at the neck and at the bottom for the limbs.

The bio-heat model and its clothed segments including limbs are coupled to the clothed cylinder ventilation model in order to determine the associated boundary condition of skin temperatures to be used as inner cylinder thermal condition as mentioned earlier. This section starts with the clothed heated cylinder ventilation

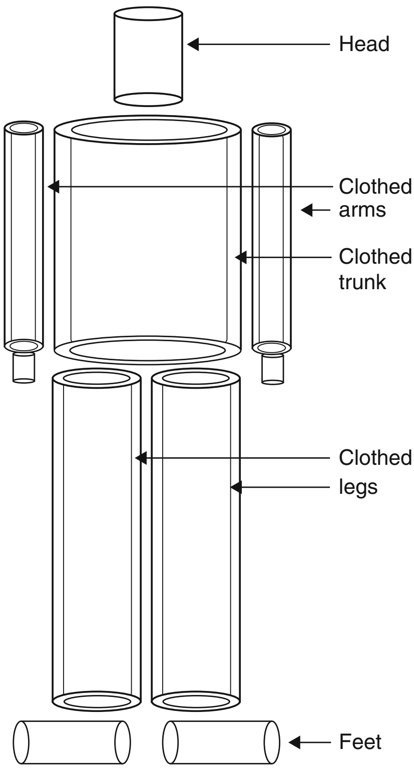

Fig. 2 The clothed human body segments

model followed by some results showing how the model can be used to predict the clothed human overall clothing ventilation and compare these predictions with published empirical findings.

4.1 Clothed Cylinder Model of Independent Body Segments

There are several challenges to modeling local ventilation based on clothed cylinder model due to the presence of clothing apertures and the microclimate air layer size. Clothing ventilation is essentially related to the flow characteristics in the air layer between skin and clothes, the clothing permeability (Lotens 1993), and on the open clothing apertures (Ghaddar et al. 2005, 2010). The flow characteristics in the trapped air layer are the results of two phenomena: natural convection associated with warm body skin and forced flow induced by both wind that penetrates permeable clothing and by flow through the opening.

The physical configuration of the present study shown in Fig. 3 consists of two concentric cylinders of radius R_s and R_f and height L. A microclimate air annulus of thickness $Y = R_f - R_s$ is trapped between the inner solid cylinder maintained at temperature T_{skin} and the outer porous cylinder represented by an isotropic fabric layer of permeability and thickness e_f. The top end of the annulus is closed and adiabatic, while the bottom end is open to the environment at temperature T_{amb}. The configuration is placed in perpendicular to an air flow at V∞. Some air penetrates

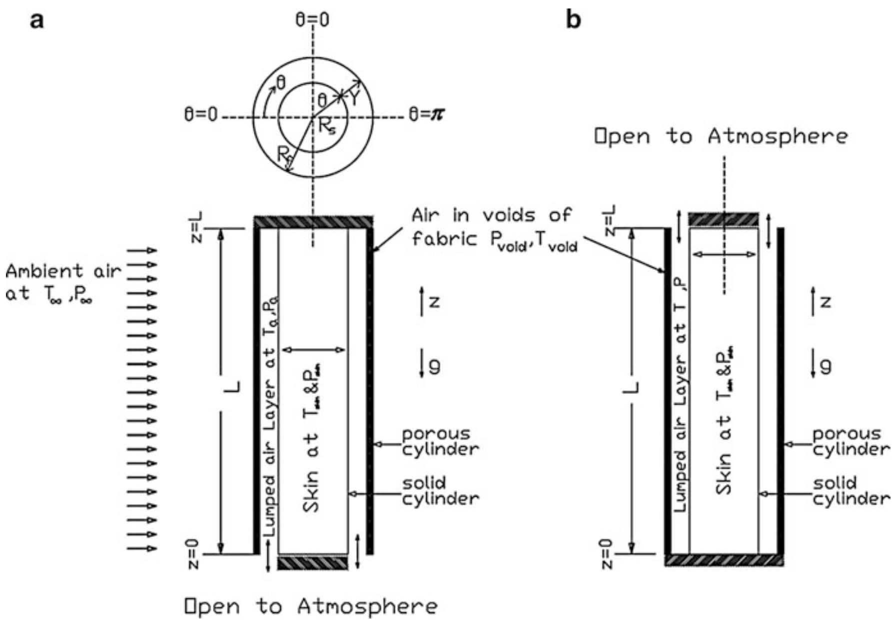

Fig. 3 Schematic of clothed cylinder with open aperture at (**a**) the *bottom* end and (**b**) *top* end

through the porous fabric into the air layer and is mixed with the incoming air from the bottom aperture at environment temperature and is then driven upward by the presence of the pressure gradient and the natural convection. The annulus trapped air thickness Y is small compared to the length L and the inner radius cylinder R_s which permits assuming Poiseuille flow in axial and angular directions even for the mixed buoyant upward flow.

The outer clothing cylinder is assumed to consist of a layer made of fibers containing air voids. Air penetrates fabric through pores and entered to the microclimate space between skin and clothing. Water vapor is assumed to diffuse through air void space to be absorbed or desorbed by fibers depending on the type of the fabric. The skin is assumed exchanging heat and moisture with the microclimate air layer and radiation heat transfer with the outer node. Thus skin is considered as an interface so that there is no storage term (transient term) to be considered. Convection takes place in the void space between penetrating air and the fabric. The flow characteristics in the air layer are the results of two phenomena: natural convection associated with warm body skin and forced-flow induced by wind effect that causes penetration of air through clothing and induced flow through the opening driven by pressure difference between ambient air and air layer (Sobera et al. 2003; Kind et al. 1991; Leong and Lai 2006). The mass and energy balances in the microclimate air layer are derived in what follows for the cylindrical geometry.

Since both ventilation through fiber and natural convection flow derived in axial direction by the open aperture, the mass conservation equation and the energy balance are coupled in the air layer and are given by

$$\frac{\partial(Y\dot{m}_{az})}{\partial z}+\frac{\partial(Y\dot{m}_{a\theta})}{R_f\partial\theta}-\dot{m}_{aY}=0 \tag{18}$$

where $\dot{m}_{az}$ is the mass flux in the vertical z-direction in kg/m^2·s, $\dot{m}_{a\theta}$ is the mass flux in the angular θ-direction, and $\dot{m}_{aY}$ is the radial infiltrating air flow rate through the fabric as defined in Eq. 7 previously.

The gap width Y and the slope *$\partial Y/(R_f\partial\theta)$ can be assumed small for clothed cylinder and* the annulus channel length πR_f is much larger width ($\pi R_f >> Y$) which justify the assumption of 1-D fully developed quasi-parallel flow in the angular direction within the annulus. This is a commonly used model in hydrodynamic lubrication theory for journal bearings (Massey 1989). So, assuming Poiseuille flow in the θ-direction, the angular air mass flow rate per unit area is expressed in terms of the annular pressure as

$$\dot{m}_{a\theta}=-\frac{Y^2}{12R_f\nu}\frac{dP_a}{d\theta} \tag{19}$$

The upward mass flow rate is expressed in terms of pressure and driving temperature gradient of the air and temperature difference between the inner wall and the infiltrating air at fabric void temperature T_{void}. The upward mass flow rate per unit area due to forced flow is given by

$$\dot{m}_{az} = -\frac{Y^2}{12v}\frac{dP_a{}^*}{dz} \tag{20}$$

$$P_a^* = P_a + \rho_a g z \tag{21}$$

while the induced buoyant mass flow rate term is

$$\dot{m}_{an} = \rho\frac{g\beta Y^2}{12v}(T_a - T_{\text{void}}). \tag{22}$$

The radial, angular, and upward mass flow rates of Eqs. 19, 20, 21, and 22 are substituted in Eq. 18 to get the mass conservation equation in pressure and temperature form as

$$\frac{\alpha\rho_a(P_a - P_s)}{\Delta P_m} + \frac{\partial}{R_f^2\partial\theta}\left(\frac{Y^3}{12v}\frac{\partial P_a}{\partial\theta}\right) + \frac{\partial}{\partial z}\left(\frac{Y^3}{12v}\frac{\partial P_a{}^*}{\partial z}\right) + \frac{\rho g\beta Y^3}{12v} \times \frac{d(T_a - T_{\text{void}})}{dz} = 0 \tag{23}$$

The steady state dry energy balance on the air spacing annulus is a balance of the dry convective heat transfer from the surface of the inner cylinder; the heat flow to the air associated with mass fluxes from the radial, angular, and upward directions; the heat diffusion from void air of the thin fabric to the air layer; and the angular conduction of heat in the air layer. The dry energy balance of the air layer is then given by

$$h_{c\,(\text{skin-air})}(T_{\text{skin}} - T_a) + h_{c-o}(T_o - T_a) + \max(\dot{m}_{ay}, 0)\ c_p\ T_{\text{void}} - \max(-\dot{m}_{ay}, 0)\ c_p\ T_a = \frac{\partial(Y.q_{\dot{m}_{az}})}{\partial z} + \frac{\partial(Y.q_{\dot{m}_{a\theta}})}{R_f\partial\theta} - \frac{k_a}{R_f^2}\frac{\partial}{\partial\theta}\left(Y\frac{\partial T_a}{\partial\theta}\right) - k_a\frac{\partial}{\partial z}\left(Y\frac{\partial T_a}{\partial z}\right) \tag{24}$$

where heat flow per gap width in z and θ directions are given by

$$\begin{aligned} q_{\dot{m}_{az}} &= \dot{m}_{az} \cdot c_p \cdot T^a \\ q_{\dot{m}_{a\theta}} &= \dot{m}_{a\theta} \cdot c_p \cdot T_a \end{aligned} \tag{25}$$

where $h_{c(\text{skin-air})}$ is the convection coefficient from the skin to the air, $h_{c(o\text{-air})}$ is the convection coefficient from the fabric to the air, T_o is the fabric outer node temperature, k_a is the thermal conductivity of air in the trapped air annulus, and c_p is the air specific heat. The values of the convective coefficients are provided in Table 1.

Table 1 Summary of convection heat transfer coefficients used in the model

Convection coefficient	Value or equation (W/m^2·K)	References
$h_{cskin-air}$	10.5	Mohanty and Dubey (1996)
h_{co}	9.6	Mohanty and Dubey (1996)
$h_{c(o-air)}$	$h_{coae} = a.V_\infty{}^b$ where $a = 4.8^* (2.R_f)^{-0.33}$ and $b = 0.5$	Danielson (1993)
h_r	3.7	Song (2007)

4.1.1 Boundary Conditions

Modeling mixed convection in small-thickness vertical annulus with open bottom lower boundary, connecting to the environment, has relatively more complex boundary condition to tackle at the opening than mixed convection with open top boundary. The complexity arises from the change in the direction of the flow (upward or downward) depending on angular position in the open annulus which requires special treatment of the boundary conditions at the opening (Patankar 1980). When the space between the two concentric cylinders is small enough, the velocity of the inlet or exit natural convection flow is only axial (Anil Lal and Reji 2009; Alarabi et al. 1987; Anil Lal and Kumar 2012). In this situation, the boundary conditions are influenced only by the pressure and temperature conditions.

Researchers identified two different types of pressure boundary condition that can be used for bottom openings. The first type is when the static pressure is equal to zero gauge pressure in both the inlet and the exit flow (Chan and Tien 1985). The second type is when the static pressure at the exit and the stagnation pressure at the inlet are equal to zero gauge pressure (Anil Lal and Reji 2009; Zamora and Hemandez 2011; Evangellos et al. 2007). Anil Lal and Kumar (2012) compared the two types and found that the second type of boundary condition is more reasonable and adequate to simulate developing natural convection flow between parallel surfaces.

For thermal boundary conditions at the inlet and outlet of an annulus, researches have assumed that the inlet fluid temperature is considered uniform and ambient. However, the gradient of the temperature of the fluid leaving the annulus is set equal to zero (Anil Lal and Reji 2009; Alarabi et al. 1987; Anil Lal and Kumar 2012). These conditions are applicable to the natural convection inflow and outflow only through one end of the annulus top or bottom.

In the presented model, the second type of pressure boundary condition is used for open aperture at the lower end of the cylinder while Bernoulli's equation is applied between P_∞ in the far environment to the opening at $z = 0$, using C_D, the loss coefficient, at the aperture of the domain dependent on area ratio of the aperture to the air layer thickness Y. The associated boundary conditions for the air flow and pressure are summarized as follows:

(a) *Aperture is z = 0 for the lower opening*:

$$\dot{m}_{az}(z=0,\theta) = C_D[2\rho_a(P_a - P_\infty)]^{1/2}; P_a(z=0,\theta) = P_\infty - \frac{[\dot{m}_{az}(z=0,\theta)]^2}{2\rho_a} \tag{26a}$$

At the closed end:

$$\dot{m}_{az}(z=L,\theta) = 0 \ \& \ \frac{dP_a((z=L,\theta)}{dz} = 0 \tag{26b}$$

(b) *Aperture is at z = L with opening at the top*:

$$\dot{m}_{az}(z=L,\theta) = C_D[2\rho_a(P_a - P_\infty)]^{1/2}; P_a(z=L,\theta) = P_\infty - \frac{[\dot{m}_{az}(z=L,\theta)]^2}{2\rho_a} \tag{26c}$$

At the closed end whether at top or bottom level:

$$\dot{m}_{az}(\theta) = 0 \quad \& \quad \frac{dP_a(\theta)}{dz} = 0 \tag{26d}$$

At the angular symmetry line:

$$\dot{m}_{a\theta}(z,\theta = 0 \ or \ \pi) = 0 \tag{26e}$$

Considering the inner cylinder as isothermal at T_{skin} and the environment temperature at T_∞, the associated thermal boundary condition use zero temperature gradient when the air is leaving or when end is closed and assumes ambient temperature when the flow is entering.

4.1.2 Microclimate Ventilation Rate and Sensible Heat Loss

Of interest is to calculate the total ventilation rate of the fabric, based on the renewal rate induced by external wind penetrating the porous fabric and enhanced by buoyancy. The total ventilation rate is calculated as the positive flow of air into the air annulus integrated per unit area of the clothed surface as follows:

The segmental sensible heat loss Q_s from the skin to the microclimate air layer used in the clothed cylinder model and bio-heat model is given by

$$\dot{m}_a(kg/s \cdot m^2) = \frac{1}{\pi L}\int_0^L\int_0^\pi \max(0, \dot{m}_{ay})\, d\theta\, dz \tag{27a}$$

$$Q_s(W) = \int\int \left(h_{c\,\mathrm{skin-air}} R_s (T_{\mathrm{skin}}(\theta, z) - T_a(\theta, z)) + h_r R_s (T_{\mathrm{skin}}(\theta, z) - T_o(\theta, z)\right) d\theta\, dz \tag{27b}$$

4.2 Bio-Heat Model Integration and Overall Clothing Ventilation

The bio-heat model (Ghali et al. 2011) is adopted in this chapter, and it divides the body into 17 segments: head, chest, back, pelvis, buttocks, lower arms, upper arms, hands, thighs, calves, and feet. The model equations simulate the heat and moisture transport from the human skin through the clothing system using a modified Gagge's model (Gagge 1973). Each body segment body is represented by Gagge's two-node model (Gagge 1973), where two energy balance equations were developed for the core node and the skin node. The sensible heat exchange from the skin to the air layer is expressed in terms of the convection heat loss at the skin surface and the radiation exchange between the skin and the fabric. The skin temperature obtained from the human body model is an input boundary condition to the clothed cylinder model. For the latent heat transfer, the boundary condition is more complex. If liquid is present on the skin surface then the skin boundary condition is the saturation pressure at the skin temperature $P_{sk} = P(T_{sk})$. The vapor pressure at the skin surface is determined by a balance between the diffusion of vapor through the skin, the sweat secreted, and the transport of moisture away from the skin as reported by Jones and Ogawa (1993). In the analysis of this chapter, it is assumed that no liquid exists at the skin surface.

The bio-heat model is coupled through the skin temperature to the proposed mixed convection model of the clothed trunk and limb segments with open apertures to estimate local ventilation rates. Local ventilation rate is an important parameter because of its effect on the clothing resistance. Therefore, the bio-heat model incorporates as input a dynamic resistance that takes into account the correction on the dry resistance due to the local ventilation as given in Eqs. 8 and 9. The most comprehensive data on dynamic clothing dry resistance originates from the work of Havenith et al. (1990) describing the changes in clothing insulation values due to motion of the wearer and wind. Ismail et al. (2014) has reported results of the coupling of bio-heat model, and clothing cylinder models and validating the model with Havenith et al. (1990) published experimental data on total clothing ventilation, vapor resistance, and permeability index for different human postures and wind velocities. Ismail et al. (2014) selected three clothing ensembles to validate the segmentally constructed ventilation and bio-heat model as follows:

- Ensemble **A** (permeable case): workpants (cotton, $\Phi = 0.66$, $\alpha = 2.121$ m/s); poly-shirt (50% polyester, 50% cotton, porosity $= 0.85$, $\alpha = 5.465$ m/s); and sweater (cotton, acrylic, porosity $= 0.82$, $\alpha = 4.13$ m/s).
- Ensemble **B** (semi-permeable): workpants (cotton); poly-shirt (50% polyester, 50% cotton); sweater (cotton, acrylic); coverall (cotton, porosity $= 0.5$, $\alpha = 2.161$ m/s).

- Ensemble **C** (impermeable): workpants (cotton); poly-shirt (50% polyester, 50% cotton); sweater (cotton, acrylic); rain coverall (nylon, porosity = 0.1, $\alpha = 2.3.10^{-3}$ m/s).

The bio-heat model of Ghali et al. (2011) was coupled through the skin boundary condition (temperature) to the clothed cylinders model. The metabolic rate was set for a standing person. The ambient conditions (temperature and humidity) and external wind velocity were also required as input to the bio-heat model. The resulting segmental ventilation rate obtained from the clothed cylinder model was entered to the bio-heat model by means of the dynamic resistance for the ventilation through fabric to predict the skin temperature. The new skin temperature was used again in the connected cylinder model to predict segmental ventilation. The alternating solution between the two models is repeated until converging skin temperature and segmental ventilation rate were obtained between the bio-heat model and the connected cylinders model.

Figure 4 presents the comparison of Ismail et al. (2014) between model predictions and experimental results of ventilation. Note that all the values predicted fell in the range of the standard deviation of the experimental study. Thus, good agreement was found between the parametric study predictions and experimental measurements of ventilation using the tracer gas. The model showed that when the wind speed increased, the opening in the bottom did not show any advantage in the drawing of the ambient air. This is due to the diminishing effect of the natural convection for wind speeds above 2.0 m/s. The effect of permeability was shown to enhance ventilation. A 36% increase in ventilation was obtained by changing from semipermeable to permeable ensemble when only natural convection was present (no wind). However, when V_∞ was larger than 2.0 m/s (forced convection), the

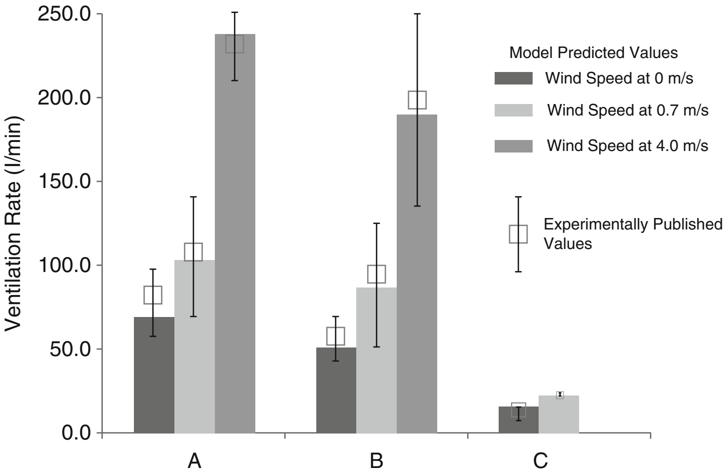

Fig. 4 Comparison between overall clothing ensemble ventilation predicted by constructed clothed human model and those of experimental results

increase in ventilation by changing from semipermeable to permeable ensemble was 24%. For higher permeability ensemble, the natural convection enhancement effect on ventilation rate is more considerable than that encountered at low permeability ensemble. Thus, the increase in permeability is indispensable to improve the ventilation in no wind condition because the natural convection enhancement effect on the flow within the air layer induces flow from ambient air due to pressure difference created between the ambient air and air within the air gap.

4.3 Connected Clothed Cylinders Model to Improve Clothing Ventilation Predictions

The ventilation model constructed from the clothed cylinder model was improved by considering the effect of clothing connection at the shoulder between the arms and the trunk. The mixed convection connected clothed cylinders model of microclimate air of the human upper body was recently developed by Ismail et al. (2015) using the physically connected clothed cylinders model of the clothed human upper body as shown in Fig. 5. The upper body connection through the shoulders was incorporated as connection element and pathway for the microclimate air flow between clothed arms and trunk. One large cylinder represented the upper shoulder level of the connected upper part of the two arms and the trunk, while three independent cylinders were extended downward from the large cylinder. Each of the arm and the trunk was formed by two co-axial annuli of different inner and outer radii. The

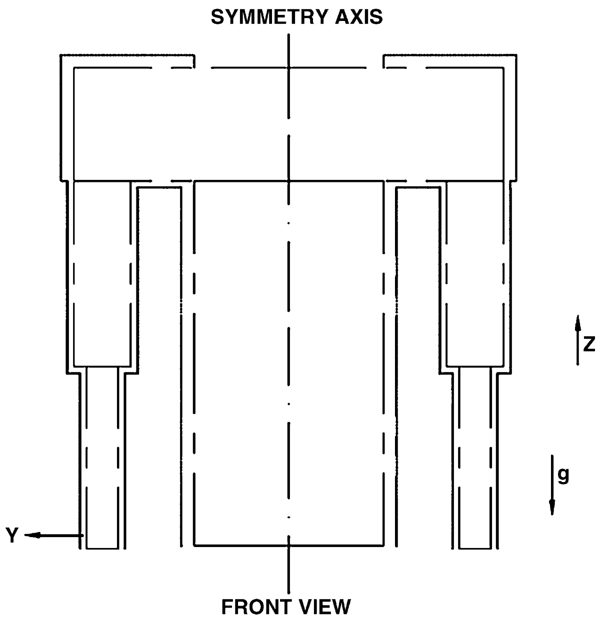

Fig. 5 Physical configuration of the upper part of the human body

inner solid cylinder represented the heated skin and the outer cylinder represented the permeable fabric. The two cylinders were separated by a microclimate air annulus where the flow and heat characteristics were modeled.

Ismail et al. (2015) derived and solved the coupled pressure equation of mass and momentum for narrow annular flow as well as the water vapor transport and energy transport equations for the microclimate air layer. They also coupled the microclimate air balance equations to the three-node fabric model described in this chapter representing the thin fabric. The interconnected cylinder model was described in the work of Ismail et al. (2015) and was validated by CFD modeling of the microclimate air geometry and by comparison to published experimental results on clothing ventilation of Ke et al. (2014) for a permeable jacket ($\alpha = 0.135$ m/s) at different wind velocities of $V_\infty \leq 0.1$ m/s (no wind), $V_\infty = 0.6$ m/s, and $V_\infty = 0.9$ m/s. The experiment was carried out on a standing shop manikin in an air-conditioned chamber at 20 °C ambient temperature and 40 ± 10% relative humidity. The dimensions used in the published experiment 3 (garment S1) are the same used in the model.

Table 2 presents the total ventilation values predicted by the connected model as compared with the published experimental values at different wind speeds for the same permeable jacket when the connection effect is included and when it is excluded. It is observed that the connected model is closer in accuracy to the published experiment (with an error not exceeding 12%) than the unconnected one (with an error exceeding 15%) at relatively high wind speeds ($V_\infty \geq 0.6$ m/s). However, it shows approximately the same result at low wind speeds ($V_\infty \leq 0.1$ m/s).

Figure 6a shows the inter-segmental ventilation using a permeable jacket ($\alpha = 0.135$ m/s) at different wind speeds. It was shown that when the velocity increases, the inter-segmental ventilation increased. At low wind speeds ($V_\infty \leq 0.1$ m/s), it was found that the inter-segmental ventilation was no longer significant. In this case, the trunk and the arm can be modeled as independent segments. However, at high wind speeds ($V_\infty \geq 0.9$ m/s), the inter-segmental ventilation exceeds 5 *l*/min. Another important factor that affects the inter-segmental ventilation is the clothing permeability. In general, the jacket permeability allows air to enter to the segmental microclimate air layers and the interconnection allows the air exchange between the segments. In order to study the impact of permeability on the inter-segmental ventilation, different jacket permeability are investigated at a wind speed of 1 m/s. Figure 6b illustrated this impact. It showed that at relatively high permeability ($\alpha = 0.135$ m/s), the inter-segmental ventilation was significant and reaches 5 *l*/min. However, at lower permeability ($\alpha = 0.05$ m/s), the connection impact vanished and the air exchange between the trunk and the arm was no longer important. The third important parameter that affects the inter-segmental ventilation is the opening at the bottom end of the lower arm and at the neck. Figure 6c illustrated this effect by showing the inter-segmental ventilation rates at different apertures. At $V_\infty = 1$ m/s and for a permeable jacket ($\alpha = 0.135$ m/s), it was found that the inter-segmental ventilation became more significant when the bottom opening of the arm was open than when it was closed. This is because the pressure at the arm microclimate air layer increases when the bottom end of the arm is closed. This pressure increase caused lower air exchange leaving the trunk to the arm. However, this was not the case

Table 2 Comparison of published experimental values (Ke et al. (2013) and predicted model ventilation values for unconnected and connected clothing model (Ismail et al. 2014, 2015) at different wind speeds

V_∞ (m/s)	0.1 m/s		0.6 m/s		0.9 m/s	
Experiment ventilation (Ke et al. 2013)	36.57 (*l*/min)		44.5 (*l*/min)		58.5 (*l*/min)	
	Ventilation (*l*/m)	Relative error (%)	Ventilation (*l*/m)	Relative error (%)	Ventilation (*l*/m)	Relative error (%)
Model connected (Ismail et al. 2015)	32.12	12.16	40.65	8.65	60.01	2.58
Model unconnected (Ismail et al. 2014)	32.54	11.02	37.79	15.07	55.09	5.82

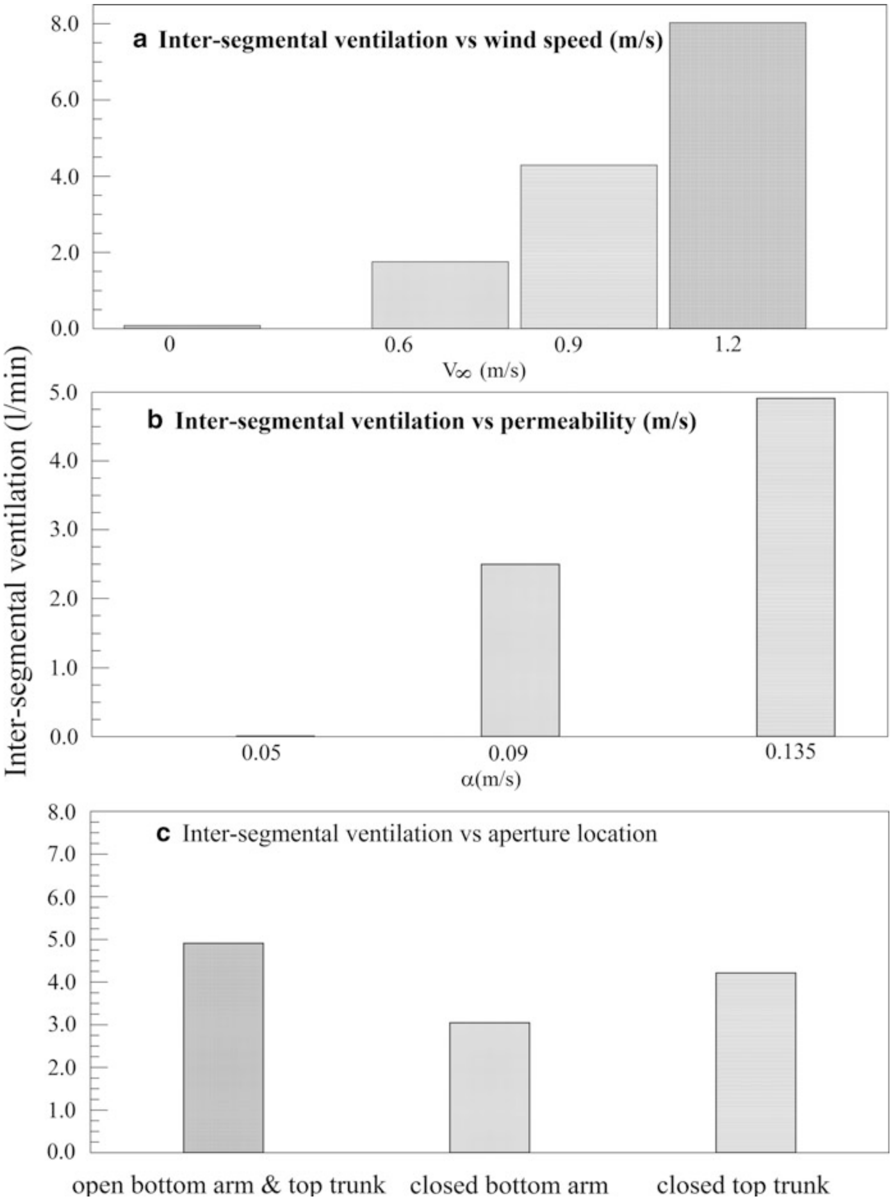

Fig. 6 Estimation of the inter-segmental ventilation obtained from the ventilation model as a function of (**a**) wind speed (**b**) permeability (**c**) apertures

when the top end of the trunk was closed. No significant variation in the inter-segmental ventilation in both cases: open top end or closed top end.

Ismail et al. (2016) performed experiments on thermal manikin with connected sleeve and trunk and unconnected clothed segments to assess the effect on associated dry heat loss at environmental conditions of 24 ± 0.5 °C and relative humidity of 40 ± 3% and wind velocity of 1.2 m/s. Figure 7 shows a comparison between their analytical and the experimental segmental ventilations for both cases of closed and open connection between clothed arm and clothed trunk of the jacket of 0.09 m/s permeability. Good agreement was reported between the analytical and experimental local ventilation rates.

Table 3 shows a comparison between the analytical prediction and experimental data of segmental ventilation and heat losses in both cases: open and closed connection for an ensemble with permeability of 0.09 m/s. Good agreement was shown between them. Closing the connection affected the segmental ventilation and heat losses for both arm and trunk. The heat losses and ventilation from the trunk decreased when the connection is closed. This is compensated by an increase of the arm ventilation and heat losses. This was due to the flow of the heated air from the trunk to the arm when the connection was opened which allowed fresh air to enter the trunk microclimate. This fresh air increased the segmental ventilation of the trunk by 12% and the heat losses by 5.46%. In the other hand, the heated air that left the trunk and entered the arm reduced the arm ventilation by 3% and reduced the heat losses by 6.68%.

As discussed earlier, the inter-segmental ventilation causes the trunk ventilation to increase by allowing some fresh air mass flow rate to penetrate instead of the heated mass flow rate (inter-segmental ventilation). Indeed, the trunk ventilation is

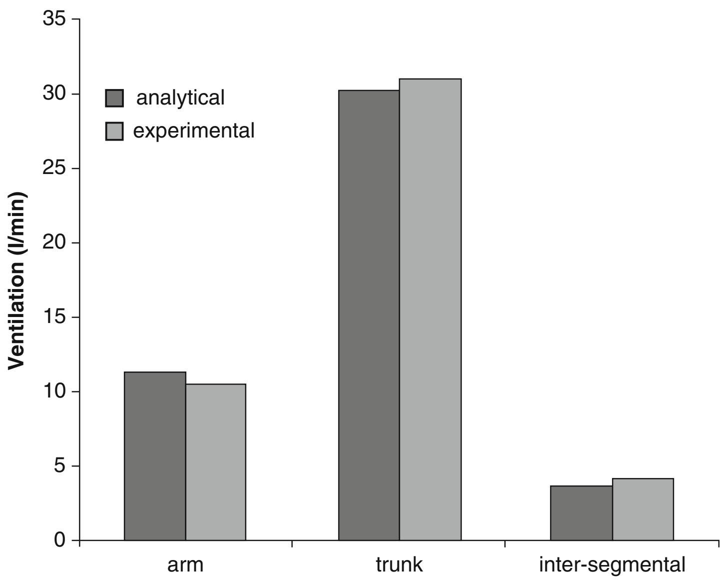

Fig. 7 Comparison between the analytical and experimental ventilations for the permeable jacket at $\alpha = 0.09$ m/s

Table 3 Comparison between the segmental ventilation and heat losses between open and closed connection (Ismail et al. 2016)

Clothed segment	Type of connection	Ventilation (*l*/min)	
Arm	Open connection	Model	11.26
		Experiment	10.56
	Closed connection	Model	12.034
		Experiment	10.856
Trunk	Open connection	Model	31.20
		Experiment	30.88
	Closed connection	Model	28.63
		Experiment	27.5
Segment	**Type of connection**	**Heat losses (W/m^2)**	
Arm	Open connection	Model	52.15
		Experiment	53.3
	Closed connection	Model	56.705
		Experiment	57.12
Trunk	Open connection	Model	64.914
		Experiment	65.4
	Closed connection	Model	59.126
		Experiment	61.536

essential in providing the human thermal comfort (Zhang 2003). The trunk is reported as the most influential segment because of its highest segmental heat loss (Zhang and Zhao 2007). Ismail et al.'s (2016) predictive model of clothing ventilation accounted for inter-segmental air exchanges between clothed arms and trunk. They found that the inter-segmental ventilation was substantial at relatively high wind speed and high clothing air permeability and should not be neglected. Moreover, they reported that accounting for the inter-segmental ventilation resulted in more accurate predictions of the overall clothing ventilation where the relative error between the predicted and published experimental overall clothing ventilation data was reduced from 15% to 8% at relatively high wind speed and air permeability.

4.4 Effect of Walking on Ventilation and the Clothed Swinging Arm Model

Clothing microclimate ventilation is modeled for the condition when the human is subject to external wind that penetrates through the fabric or ensemble openings. These predictive models are presented in the previous subsections using connected clothing cylinder models integrated with bio-heat models with the assumption that both the limbs and trunk are subject to the same wind conditions and may not be applicable to the more complex physical situation due to wearer displacement causing relative motion of clothed body parts (limbs) with respect to their clothing cover. During walking, ventilation is not uniform over the clothed human body. The trunk local ventilation is different than ventilation induced by swinging motion of limbs at small or large swinging amplitudes and frequencies (Ghali et al. 2002c). Different body parts during walking are subject to different mechanisms of wind, swinging motion, and combined wind and swinging motion that stimulate ventilation at different rates. When different segments have different ventilation rates, local thermal comfort evaluated by skin wittedness and comfort sensation becomes important in assessing whole body comfort. The standard ISO-7730 (2005) requires determination of clothing insulation of active persons or persons exposed to significant wind. Data on dynamic insulation have limited use since they are applicable for the specific ensembles, activity levels, and experimental conditions used in generating them.

Most of the research on clothing ventilation of walking humans was empirical and few studies dealt with the mechanism of microclimate ventilation by wind and motion through modeling. Previous work of Ghali et al. (2009) and Ghaddar et al. (2008) addressed the effect of the changing gap width induced by an oscillating body part (cylinder) within a fixed single clothing cover at uniform external environment pressure with close and open clothing apertures. A clothed swinging arm model was developed by Ghaddar et al. (2008). The developed model was capable of estimating the renewal flow rates for general limb motion configuration taking into consideration the periodic motion of the limbs and clothing, their geometric interaction at skin-fabric contact or no contact, open or closed clothing apertures, and in presence of wind or no wind. However, the model assumed the clothed swinging arm as an independent segment that is not connected with the trunk as shown in Fig. 8. They used the swinging clothed arm model to determine the dynamic clothed limb resistance in a follow-up work by Ghali et al. (2009) to predict the mean steady periodic heat loss from the clothed cylinder using Lotens' simple heat resistance network model and validated their model with experiments (Lotens 1993). They reported that the use of lumped dry and evaporative heat resistance network that accounted for the effect of ventilation through clothing fabric and clothing opening resulted in relatively good predictions of heat loss from the a clothed swinging solid cylinder in the presence of wind. The use of accurate ventilation rates is an important input to the simplified thermal model using dynamic resistance. The ventilation through clothing by wind and motion was also reported to double or triple heat loss as compared to the case of still cylinder in quiet air.

The clothed swinging limb model is still lacking the interconnection effect during walking between clothed trunk and arms and to determine whether interconnection air follows enhances trunk or limb ventilation in similar way to static clothed cylinder interconnection. This remains subject of future research to have a versatile and complete ventilation model of clothed human. Such a model can be used to estimate accurately human heat losses and assess human thermal comfort under different climate conditions and activity level.

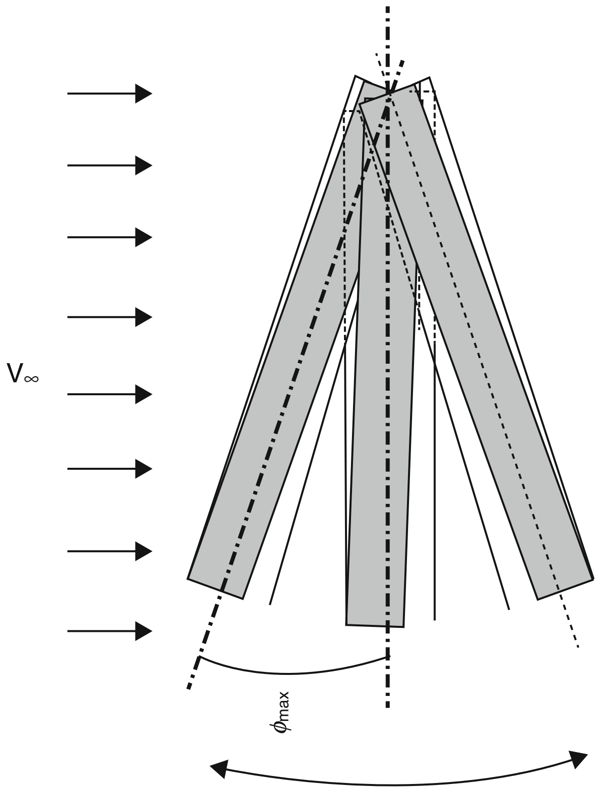

Fig. 8 Representation of the human limb motion inside the clothing cylinder

5 Closing Remarks and Future Trends

Ventilation is an important design parameter for summer weather clothing of active people to increase heat loss from the human body. Based on research work done for modeling and predicting clothing ventilation, enhancement of microclimate exchanges between different body segments is desirable in garment design. Walking ventilates moving arms and legs. Clothed trunk ventilation can be enhanced with larger microclimate air exchange permitted between body segments to channel the airflow from the relatively high-ventilated limbs microclimate to the less-ventilated trunk microclimate.

Ventilation of the microclimate air layer is an attractive solution for design of versatile clothing for active people that could result in enhancing effectiveness of moisture removal away from the skin. Ventilation rates can be altered where needed by the proper choice of fabric permeability, arrangement of clothing layers, reducing internal microclimate flow resistance for internal air exchanges between connected clothed body segments, and aperture positions, size, and operational flexibility of controlling the extent of microclimate air direct connection with the environment.

Extensive research is still needed to understand the relationship between segmental ventilation and local discomfort during walking and when subject to wind for optimizing active wear designs. Inter-segmental air exchanges modeling is target of future work to complete the clothed human thermal model based on physiology and first principles. Moreover, development of models that predict liquid moisture transport in fabric is also needed to allow extending the clothed human model to high activity rate where moisture wicks the fabric and moves to outer layers depending on gradients of temperature between skin and environment. Such models would be useful for predicting the human thermal stress state and endurance at high activity level.

6 Cross-References

► Analytical Methods in Heat Transfer
► Applications of Flow-Induced Vibration in Porous Media
► Electrohydrodynamically Augmented Internal Forced Convection
► Full-Coverage Effusion Cooling in External Forced Convection: Sparse and Dense Hole Arrays
► Heat Transfer Media and Their Properties
► Macroscopic Heat Conduction Formulation
► Single-Phase Convective Heat Transfer: Basic Equations and Solutions
► Thermophysical Properties Measurement and Identification

References

Alarabi M, El-Shaarawi MAI, Khamis K (1987) Natural convection in uniformly heated vertical annuli. Int J Heat Mass Tran 30(7):1381–1389

American Society for Testing and Materials (1965) ASTM D-39-49. ASTM D39-65 Method of test for construction characteristics of woven fabrics

American Society for Testing and Materials (1983) ASTM D737-75, Standard test method for air permeability of textile fabrics, (IBR) approved 1983

American Society for Testing and Materials (1985) ASTM D1518: Standard test method for thermal resistance of batting systems using a hot plate

American Society for Testing and Materials, ASTM D737-96 (2012) Air permeability. Standard test method for air permeability of textile fabrics, ASTM Organization

American Society of Heating, Refrigerating and Air-Conditioning Engineers (2005) ASHRAE handbook of fundamentals. ASHRAE, Atlanta

Anil Lal S, Kumar A (2012) Numerical prediction of natural convection in a vertical annulus closed at top and opened at bottom. Heat Tran Eng 33(15):70–83

Anil Lal S, Reji C (2009) Numerical prediction of natural convection in vented cavities using restricted domain approach. Int J Heat Mass Transf 52:724–734

Chan YL, Tien CL (1985) A numerical study of two dimensional laminar natural convection in shallow open cavities. Int J Heat Mass Transf 28:603–612

Chatterjee PK (1985) Absorbency. Elsevier Science Publishing Company, Amsterdam

Danielson U (1993) Convection coefficients in clothing air layers. Doctoral thesis, The Royal Institute of technology, Stockholm
Evangellos B, Vrachopoulos M, Koukou M, Margaris D, Filios A, Mavrommatis S (2007) Study of the natural convection phenomena inside a wall solar chimney with one wall adiabatic and one wall under a heat flux. App Therm Eng 27:226–234
Farnworth B (1986) A numerical model of combined diffusion of heat and water vapor through clothing. Text Res J 56:653–655
Fourt L, Hollies NRS (1970) Clothing: comfort and function. Martin Dekker, New York
Gagge AP (1973) A two node model of human temperature regulation in FORTRAN. In: Parker JF, West VR (eds) Bioastronautics data, 2nd edn. NASA, Washington, DC
Ghaddar N, Ghali K, Harathani J (2005) Modulated air layer heat and moisture transport by ventilation and diffusion from clothing with open aperture. ASME Heat Transf J 127(3):287–297
Ghaddar N, Ghali K, Jreije B (2008) Ventilation of wind-permeable clothed cylinder subject to periodic swinging motion: modeling and experimentation. J Heat Transf 130:1107–2020
Ghaddar N, Ghali K, Othmani M, Holmer I, Kuklane K (2010) Experimental and theoretical study of ventilation and heat loss from clothed vertical isothermally-heated cylinder in uniform flow field. J Appl Mech 77(3):1–8
Ghali K, Ghaddar N, Bizri M (2011) The influence of wind on outdoor thermal comfort in the city of Beirut: a theoretical and field study. Int J HVAC R res 17(5):813–828
Ghali K, Ghaddar N, Jones B (2002a) Empirical evaluation of convective heat and moisture transport coefficients in porous cotton medium. J Heat Transf 124(3):530–537
Ghali K, Ghaddar N, Jones B (2002b) Multi-layer three-node model of convective transport within cotton fibrous medium. J Porous Media 5(1):17–31
Ghali K, Ghaddar N, Jones B (2002c) Modeling of heat and moisture transport by periodic ventilation of thin cotton fibrous media. Int J Heat Mass Transf 45(18):3703–3714
Ghali K, Jones B, Tracy J (1994) Experimental techniques for measuring parameters describing wetting and wicking in fabrics. Text Res J 64:106–111
Ghali K, Jones B, Tracy J (1995) Modeling heat and mass transfer in fabrics. Int J Heat Mass Transf 38:13–21
Ghali K, Othmani M, Jreije B, Ghaddar N (2009) Simplified heat transport model of wind permeable clothed cylinder subject to swinging motion. Text Res J 79:1043–1055
Harnett PR, Mehta PN (1984) A survey and comparison of laboratory test methods for measuring wicking. Text Res J 54(7):471–478
Havenith G, Heus R, Lotens WA (1990) Resultant clothing insulation: a function of body movement, posture, wind clothing fit and ensemble thickness. Ergonomics 33(1):67–84
Havenith G, Holmér I, Parsons KC, Den Hartog E, Malchaire J (2000) Calculation of dynamic heat and vapor resistance. Environ Ergon 10:125–128
Henry HPS (1939) Diffusion in absorbing media. Proc R Soc 171A:215
Ismail N, Ghaddar N, Ghali K (2014) Predicting segmental and overall ventilation of ensembles using an integrated bio-heat and clothed cylinder ventilation models. Text Res J 84:2198–2213
Ismail N, Ghaddar N, Ghali K (2016) Theoretical and experimental estimation of inter-segmental clothing ventilation and impact on human segmental heat losses. In: Proceedings of ASME IMECE2015-50255E, Houston, Nov 2015
Ismail N, Ghaddar N, Ghali K (2016) Effect of inter-segmental air exchanges on local and overall clothing ventilation. Text Res J 86(4):423–439
ISO 11092 (EN31092) (1993) Textiles-physiological effects - Measurement of thermal and water-vapor resistance under steady-state conditions (sweating guarded-hotplate test)
ISO 7730 (2005) Ergonomics of the thermal environment - Analytical determination and interpretation of thermal comfort using calculation of the PMV and PPD indices and local thermal comfort criteria
Jones BW, Ogawa Y (1993) Transient interaction between the human and the thermal environment. ASHRAE Trans 98(1):189–195

Ke Y, Havenith G, Li J, Li X (2013) A new experimental study of influence of fabric permeability, clothing sizes, openings and wind on regional ventilation rates. Fibers Polym 14:1906–1911

Ke Y, Havenith G, Zhang X, Li X, Li J (2014) Effects of wind and clothing apertures on local clothing ventilation rates and thermal insulation. Text Res J 84:941–952

Kind RJ, Jenkins JM, Seddigh F (1991) Experimental investigation of heat transfer through wind-permeable clothing. Cold Reg Sci Technol 20:39–49

Leong JC, Lai FC (2006) Natural convection in a concentric annulus with a porous sleeve. Int J Heat Mass Transf 49:3016–3027

Li Y, Holcombe BV (1992) A two-stage sorption model of the coupled diffusion of moisture and heat in wool fabrics. Text Res J 62(4):211–217

Lotens W (1993) Heat transfer from humans wearing clothing, doctoral thesis. TNO Institute for Perception, Soesterberg

Massey BS (1989) Chapter 6. In: Mechanics of fluids, 6th edn. Springer, New York

McCullough EA, Jones BW, Huck J (1985) A comprehensive data base for estimating clothing insulation. ASHRAE Trans 91:29–47

McCullough EA, Jones BW, Tamura T (1989) A data base for determining the evaporative resistance of clothing. ASHRAE Trans 95(2):316–328

Minkowycz WJ, Haji-Shikh A, Vafai K (1999) On departure from local thermal equilibrium in porous media due to a rapidly changing heat source: the sparrow number. Int J Heat Mass Transf 42:3373–3385

Mohanty AK, Dubey MR (1996) Buoyancy induced flow and heat transfer through a vertical annulus. Int J Heat Mass Transf 39(10):2087–2093

Morton WE, Hearle LW (1975) Physical properties of textile fibers. Heinemann, London

Nordon P, David HG (1967) Coupled diffusion of moisture and heat in hygroscopic textile materials. Int J Heat Mass Transf 10(7):853–866

Othmani M, Ghaddar N, Ghali K (2008) An angular multi-segmented human bio-heat model to assess local segment comfort in transient and asymmetric radiative environment. Int J Heat Mass Transf 51(23–24):5522–5533

Patankar SV (1980) Numerical heat transfer and heat flow. Hemisphere Publishing Corporation, McGraw Hill Book Company, New York

Rees WH (1941) The transmission of heat through textile fabrics. J Text Inst 32:149–165

Sobera MP, Kleijn CR, Brasser P, Van den Akker HEA (2003) Convective heat and mass transfer to a cylinder sheathed by a porous layer. AICHE J 49:3018–3028

Song G (2007) Clothing air gap layers and thermal protective performance in single layer garment. J Ind Text 36(3):193–204

Woodcock A (1962) Moisture transfer in textile systems, part I. Text Res J 32:628–633

Zamora B, Hernandez J (2011) Influence of upstream conduction on the thermally optimum spacing of isothermal, natural convection-cooled vertical plate arrays. Int Comm Heat Mass Transf 28 (2):201–210

Zhang H (2003) Human thermal sensation and comfort in transient and non-uniform thermal environments. PhD thesis, University of California, Berkeley

Zhang Y, Zhao R (2007) Effect of local exposure on human responses. Build Environ 42:2737–2745